TELKOMNIKA, Vol.11, No.1, January 2013, pp. 458~467
ISSN: 2302-4046

Thermal Analysis in Gas Insulated Transmission Lines Using an Improved Finite-Element Model

Xiaowen Wu*, Naiqiu Shu, Hongtao Li, Ling Li
School of Electrical Engineering, Wuhan University
No.8, Donghu South Road, Wuchang District, Wuhan 430072, China
*Corresponding author, e-mail: whuwxw@yahoo.cn

Abstract

In this paper, an improved finite element (FE) model is proposed to investigate the temperature distribution in gas insulated transmission lines (GILs). The solution of joule losses in eddy current field analysis is indirectly coupled into fluid and thermal fields. As is different from the traditional methods, the surrounding air of the GIL is involved in the model to avoid constant convective heat transfer coefficient, thus multiple species transport technique is employed to deal with the problem of two fluid types in a single model. In addition, the temperature dependent electrical and thermal properties of the materials are considered. The steady-state and transient thermal analysis of the GIL are performed separately with the improved model. The corresponding temperature distributions are compared with experimental results reported in the literature.

Keywords*: improved finite element (FE) model, temperature distribution, eddy current field, fluid and thermal field, multiple species transport*

1. Introduction

As an alternative to overhead lines and synthetic cables, the gas insulated transmission lines (GILs) provide a technical solution for high power transmission over long distances. In addition to the advantage of comparable power transmission capability with the overhead lines, the GILs have lower resistive losses and lower capacitive load because of large cross section of the conductor and enclosure and the gaseous dielectric [1-5]. The single-circuit GIL mainly consists of three single-phase encapsulated aluminum tubes, which are possibly buried in the ground, laid in the tunnel or installed above ground.

The rate current in the conductor of GIL ranges from 1 to 40 kA in most cases. The induced current in the enclosure has the same order of magnitude. Therefore, large joule losses will be generated. Because the ampacity of the current-carrying conductor is limited by the maximum operating temperature, it is important to address the thermal problems when designing the GILs. Hitherto, several studies have been performed to determine the temperature rise of gas-insulated power apparatus with similar structure. Analytical methods which rely on empirical curves and energy balance iterations on each of the components are most commonly used in engineering [6, 7]. They are suitable for preliminary calculation of steady-state problems, but not sufficient when transient thermal analysis is needed, taking into account the temperature dependent electrical and thermal properties of the materials [8]. Recently, the finite element methods (FEM) are popular for the solution of coupled electromagnetic and thermal fields. The power losses calculated in the magnetic field analysis are used as input data for thermal analysis. Nusselt number is introduced to determine constant convective heat transfer coefficient on the surface of the enclosure [9-15]. To some degree, this method is a little inaccurate, for the coefficient is actually temperature dependent and variant at different locations of the enclosure surface. Moreover, the temperature dependent thermal properties of materials, which have a large influence on the temperature rise, are rarely mentioned in those studies.

The object of this paper is to present an improved finite element (FE) model which enables the investigation of the steady state and transient heat transfer characteristics of the GIL above ground. The important factors influencing such characteristics are considered, and

Received September 1, 2012; Revised December 5, 2012; Accepted December 13, 2012

the actual convective heat transfer coefficient is attained in the model. The predicted temperatures are validated against experimental results reported in the literature.

2. Electromagnetic Field Formulation

Each tube of the GIL is composed of the aluminum enclosure and conductor, epoxy resin insulators, the particle trap and the insulating gas (SF_6). The following assumptions have been used in the solution procedure:

- The GIL is long enough, so the end effect is ignored.
- The insulators and the particle trap are excluded in the solution region, so that the problem becomes a two-dimensional one.
- Displacement current is neglected because of the low frequency.
- The conductivity is temperature dependent.

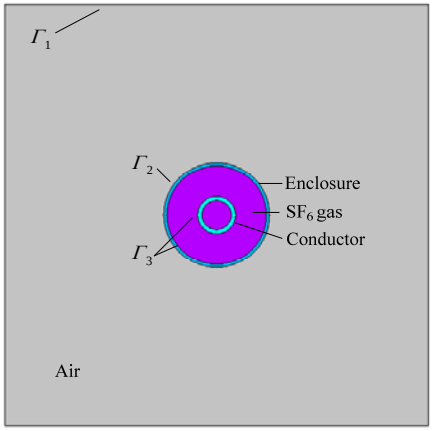

Figure 1. Solution region of the GIL

Based on the above assumptions, the magnetic vector potential and the current density have only the axial ***z*** component. The eddy current diffusion problem over the solution region, as shown in Figure 1, can be described by [11]

$$\begin{cases} \Omega : \dfrac{1}{\mu}\left(\dfrac{\partial^2 \boldsymbol{A}}{\partial x^2}+\dfrac{\partial^2 \boldsymbol{A}}{\partial y^2}\right) = j\omega\sigma(\theta)\boldsymbol{A}-\boldsymbol{J}_s \\ \Gamma_1 : \boldsymbol{A}=0 \end{cases} \tag{1}$$

and

$$-j\omega\sigma(\theta)\boldsymbol{A}+\boldsymbol{J}_s=\boldsymbol{J} \tag{2}$$

$$\iint_S \boldsymbol{J}d\boldsymbol{s}=I \tag{3}$$

where μ is permeability, $\boldsymbol{A}$ is magnetic vector potential, ω is the angular frequency, σ is electrical conductivity, θ is Celsius temperature, $\boldsymbol{J}_s$ is the uniformly distributed source current density, Ω is the solution region, Γ_1 is the outer boundary (the Dirichlet boundary condition), $\boldsymbol{J}$ is the total current density, S is the cross section of the conductor or the enclosure and I is the measured current.

The temperature dependent conductivity is approximated by

$$\sigma(\theta)=\frac{\sigma_{20}}{1+0.004(\theta-20)} \tag{4}$$

where σ_{20} is the conductivity at 20.

Applying the FEM, the power loss per unit length in the conductor and or in the enclosure can be calculated as follows:

$$Q = \sum_{i=1}^{N} q_i = \sum_{i=1}^{N} \frac{J_i J_i^*}{\sigma_i} \quad (5)$$

where N is the element number. q_i, J_i and σ_i are the power loss, total current density and conductivity of the ith element respectively.

Equation (5) is used as the volumetric heat source for the thermal problem.

3. Thermal Field Modeling

All the power losses generated in the conductor and the enclosure are converted into heat which is dissipated to the surrounding air via several stages due to the temperature difference at the boundaries of the components. The first stage of heat transfer begins from the interior of the conductor to the outer surface by heat conduction. The second stage is the transfer of heat from the conductor surface to the insulating gas by natural convection and to the interior surface of the enclosure by surface to surface radiation. The third stage is the transfer of heat from the insulating gas and the outer surface of the conductor to the interior surface of the enclosure. In this stage, the heat transfer mechanism is the same as that of the second one. In the fourth stage, the heat is transferred from the interior surface of the enclosure to the external surface by heat conduction. The last stage is the heat dissipation from the external surface of the enclosure to the surrounding air by natural convection and radiation.

To facilitate the analysis, the theoretical thermal model of the GIL is limited by the following basic assumptions:

- The effects of wind and solar radiation are ignored.
- The radiation effect of the insulating gas is disregarded.
- The insulating gas is incompressible.
- The density, dynamic viscosity and thermal conductivity of the insulating gas and air are temperature dependent, while the specific heat is considered constant.
- The outermost boundary of the solution region is far enough from the exterior of the enclosure, where the temperature is not influenced by the GIL.

3.1. Multiple Species Transport

In the traditional thermal models, great effort has been made to calculate the convective heat transfer coefficient on the enclosure surface. It is difficult to determine the coefficient, because it varies with many factors, such as the surface temperature, location and fluid velocity. To avoid the calculation of convective heat transfer coefficient, the surrounding air is also included in the solution region. Because two fluids exist in one FE model, the multiple species transport technique is employed, in which the surrounding air and insulating gas are considered as two species of some mixture. The thermal properties of this mixture are the linear combination of that for the two fluids.

The relationship between the density and the temperature of the insulating gas or the surrounding air is

$$\rho = \rho_0 \frac{P}{k_1} \frac{k_2}{T} \quad (6)$$

where T is the Kelvin temperature, ρ_0 is the fluid density at room temperature, P is the pressure, k_1 and k_2 are constants.

According to Sutherland's law [16], the thermal conductivity and dynamic viscosity of the insulating gas or the air are given by

$$\lambda = \lambda_0 \left(\frac{T}{k_1}\right)^{1.5} \frac{k_1 + k_2}{T + k_2} \quad (7)$$

$$\mu = \mu_0 (\frac{T}{k_1})^{1.5} \frac{k_1 + k_2}{T + k_2} \tag{8}$$

where λ_0 and μ_0 are the thermal conductivity and dynamic viscosity at room temperature separately.

As for conjugate heat transfer problem including multiple fluids with different properties, a single momentum equation is solved for the flow field. The properties for this equation are calculated from those of the species fluids and their respective mass fractions:

$$\alpha_{\mathrm{f}} = \sum_{i=1}^{2} Y_i \alpha_i \tag{9}$$

$$\sum_{i=1}^{2} Y_i = 1 \tag{10}$$

where α_{f} is the density, dynamic viscosity, thermal conductivity or the specific heat of the mixture, Y_i is the mass fraction of the ith species.

3.2. Fluid and Thermal Equations

The motion of the insulating gas and air is driven by the buoyancy and gravity. Thus, natural convection occurs in the fluid region. The governing equations of convective heat transfer are composed of the continuity equation, the momentum equation and the energy equation, which can be generally described as [17]

$$\frac{\partial \rho_{\mathrm{f}}}{\partial t} + \nabla \cdot \left(\rho_{\mathrm{f}} \mathbf{u} \right) = 0 \tag{11}$$

$$\rho_{\mathrm{f}} (\frac{\partial \mathbf{u}}{\partial t} + \mathbf{u} \cdot \nabla \mathbf{u}) = -\nabla P + \mu_{\mathrm{f}} \nabla^2 \mathbf{u} + \mathbf{f} \tag{12}$$

$$\frac{\partial}{\partial t} (\rho_{\mathrm{f}} C_{\mathrm{f}} T) + \nabla \cdot (\rho_{\mathrm{f}} \mathbf{u} C_{\mathrm{f}} T) = \nabla \cdot (\lambda_{\mathrm{f}} \nabla T) + Q \tag{13}$$

where **u** is the velocity vector, **f** is the vector of body forces, C_p is the specific heat and Q is the heat source generated in the conductor and the enclosure.

In the traditional approaches, as a boundary condition, convective heat transfer coefficient is applied at the interface of the enclosure and the surrounding air. This boundary is avoided in the proposed model, because the convective heat transfer is solved by the governing equations mentioned above. According to Newton's law of cooling, the convective heat transfer coefficient is presented as

$$h = \frac{q}{T_{\mathrm{w}} - T_{\mathrm{f}}} \tag{14}$$

where q is the heat flux, T_{w} is the surface temperature of the enclosure and T_{f} is the temperature of the surrounding air.

Considering the velocity in the solid region is zero, the heat conduction in the conductor and the enclosure is the simplified form of (13), which can be given by

$$\frac{\partial}{\partial t} (\rho_{\mathrm{f}} C_{\mathrm{f}} T) = \nabla \cdot (\lambda_{\mathrm{f}} \nabla T) + Q \tag{15}$$

At the outermost surface of the solution region, the boundary conditions is

$$T|_{\Gamma_1} = T_0 \tag{16}$$

where T_0 is the ambient temperature.

The velocity constraint at the solid-fluid interface and the boundary of the solution region is given by

$$\mathbf{u}|_{\Gamma_1, \Gamma_2, \Gamma_3} = \mathbf{0} \tag{17}$$

In addition to convection, there is radiant energy exchange between the conductor and the enclosure and between the enclosure and its surroundings. The heat transfer by radiation is found to have large effects on the temperature rise of the whole GIL. The mathematical formulation of the radiation boundary condition is obtained by considering an energy balance at the surface stated as [18]

$$-\lambda \frac{dT}{dx} - \lambda \frac{dT}{dy}\bigg|_{\Gamma_2, \Gamma_3} = \sigma \varepsilon F_{ij} (T_i^4 - T_j^4) \tag{18}$$

where σ is Stefan-Boltzmann constant, ε is the emissivity of the surface and F_{ij} is the view factor, which is defined as the fraction of the heat radiation from the surface A_i intercepted by the surface A_j. It can be obtained by the following equation:

$$F_{ij} = \frac{1}{A_i} \int_{A_i} \int_{A_j} \frac{\cos\theta_i \cos\theta_j}{\pi r^2} \mathrm{d}A_i \mathrm{d}A_j \tag{19}$$

where A_i and A_j are element areas, r is the distance between the two elements, θ_i and θ_j are the polar angles formed by the radiation line and the normal of the two elements.

4. FEM Solution of Electromagnetic and Thermal Problems

The FEM divides the solution region into finite regions called elements. On each element, the governing equations of electromagnetic and thermal fields are performed. Considering the loads and constraints, an assembly process results in a set of equations, in which the variants are the degree of freedom at the corners or on the edges of the elements. Linking together the solution of these equations, the interested electromagnetic and thermal behaviors of the GIL are approximated.

Two units of the GIL are separately used to investigate the steady-state and transient temperature rise characteristics of the GIL. The dimensions of the GIL are given in Table 1.

Table 1. Dimensions and Materials of the GIL

Item		Inner diameter (mm)	Thickness (mm)	Material
Unit 1	Conductor	140	20	A6063-T5
	Enclosure	470	15	A6063-T5
Unit 2	Conductor	140	20	A6063-T5
	Enclosure	480	12	A6063-T5

The whole solution region is divided into 70560 elements and 197905 nodes. As the conductivities of the conductor and the enclosure are temperature dependent, an iterative method must be used. This process is illustrated in Figure 2. The ambient temperature is initially used to calculate the power losses, and the results are coupled to fluid and thermal model in which the temperature distribution is obtained and the initial temperature is updated. The temperatures are not fixed until the error is less than 5%.

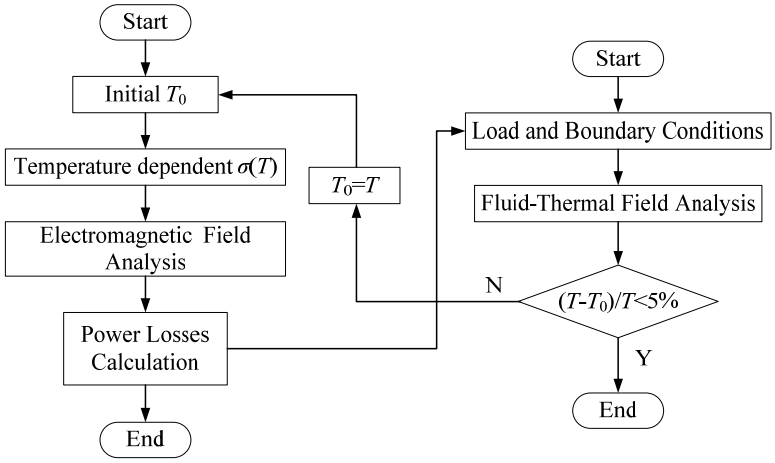

Figure 2. Flow chart of electromagnetic and thermal field analysis

4.1. Steady-State Performance

Unit 1 of the GIL is used to investigate the steady-state temperature rise characteristics. The operating frequency is 50Hz. Power loss in the conductor Q_c and power loss in the enclosure Q_e for different loading currents are reported in Table 2.

Table 2. Power Losses for Different Loading Currents

Current (A)	Q_c (W/m)	Q_e (W/m)
5000	108.79	38.31
7000	222.24	77.80
8000	297.60	103.61

The steady-state analysis determines the temperature distribution under constant load current and ambient temperature, in which the heat storage effect varying over a period of time can be ignored. Corresponding to the rated load currents 5000 A, 7000 A and 8000 A in the conductor and the enclosure, the ambient temperatures are separately 21.5 □, 23 □ and 25 □. The SF_6 gas pressure is 0.35MPa. The emissivity coefficients are chosen to be 0.9 on the inner surface of the enclosure, and 0.8 on the outer surface of the conductor [7]. The required thermal properties for each different material are listed in Table 3.

Table 3. Material Properties of the GIL

Item	ρ (kg/m^3)	λ (10^{-2} W/(m·K))	μ (10^{-5} Pa·s)	C_p (J/(kg·K))
Conductor	2730	220	0	880
Enclosure	2730	220	0	880
SF_6 gas	22.82	1.206	1.42	665.18
Air	1.293	2.44	1.72	1005

Figure 3 shows the contour plot for a nodal temperature distribution of the whole solution region at the current of 8000 A. It can be observed that the temperature is symmetrically distributed and the hottest spot, located at the conductor, is 84.3.

The temperature distribution inside the GIL is illustrated in Figure 4. Because of the high thermal conductivity, little discrepancy is found in the conductor and the conductor is considered isothermal. The temperature of the upper part of the GIL is higher than that of the lower part. This is attributed to the fact that heated SF_6 gas in the upper part rise up under the effect of buoyancy. In this case, the heat generated in the conductor is dissipated by convection and radiation. While in the lower part, the SF_6 gas is nearly static, in addition to radiation the internal

cooling is by conduction, which is less efficient than heat convection. The minimum temperature, located at the bottom of the enclosure, is 51.

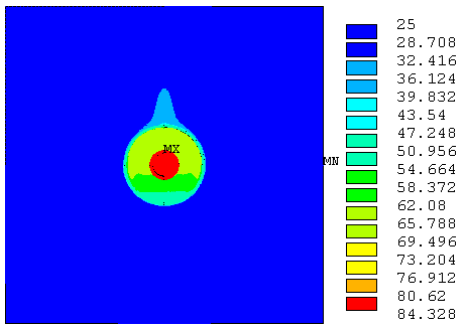

Figure 3. Temperature distribution of the solution region

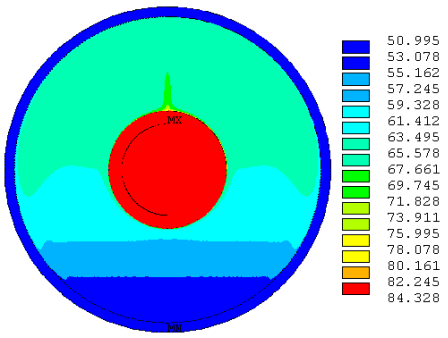

Figure 4. Temperature distribution of the GIL

For the loading current of 5000 A and 7000 A, the GIL has similar temperature distribution. The calculated results of the conductor temperature and the enclosure temperature at the top are given in Table 4. A comparison of the test results reported in [7] with the calculation results using the proposed method in this paper highlights a satisfactory agreement.

Table 4. Comparison of Test and Calculation Results

Current (A)	Conductor		Enclosure	
	Tested (□)	Calculated (□)	Tested (□)	Calculated (□)
5000	50.0	48.6	34.0	34.5
7000	72.0	72.3	47.5	47.7
8000	85.5	84.3	55.0	53.8

As it is mentioned above, the convective heat transfer coefficient varies at different locations of the enclosure surface. The actual coefficient is calculated and the distribution along the enclosure surface is shown in Figure 5. It can be observed that the maximum value, located at the bottom of the enclosure, is 4.125 W/(m^{-2}·K^{-1}), the minimum value, located at the top of the enclosure, is 1.785 W/(m^{-2}·K^{-1}).

To prove that the proposed model is more accurate than the traditional methods, it is compared with analytical method, the FEM using constant convective heat transfer coefficient (FEM-CH) and the FEM using constant material properties (FEM-CP). In the analytical method and FEM-CH, the Nusselt number is employed to calculate the convective heat transfer coefficient which is 3.138 W/(m^{-2}·K^{-1}). In the FEM-CP, the properties listed in Table 3 are used. The comparison results are shown in Figure 6. It is believed that the proposed method is much

closer to the experimental results than other approaches, and that the temperature dependent material properties are necessary to be considered.

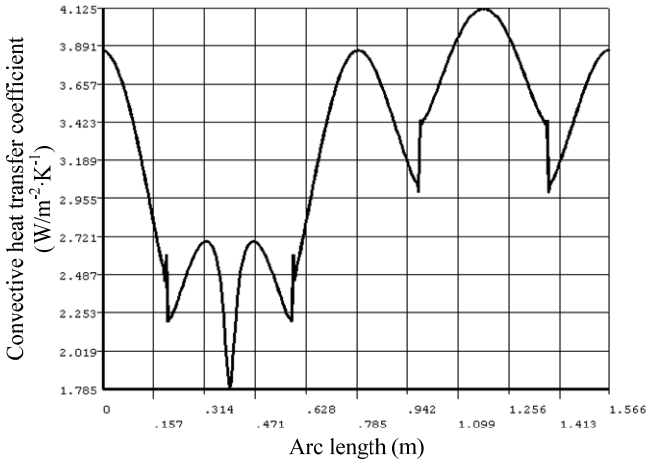

Figure 5. Convective heat transfer coefficient distribution along the enclosure surface

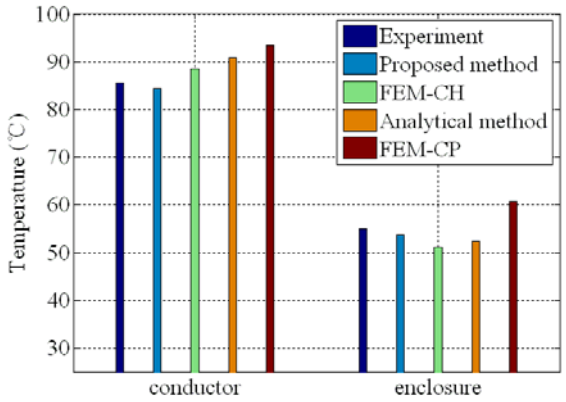

Figure 6. Comparison of the proposed and other traditional methods

4.2. Transient Performance

Transient thermal analysis determines temperatures that vary over time. It follows the same procedure as a steady-state thermal analysis. The main difference is that the most applied loads in a transient analysis are functions of time. The steady-state solution is used to establish the initial conditions.

The unit 2 of the GIL with loading current 7300 A is used to investigate the transient thermal performance. In this unit, the operating frequency is 60Hz and the pressure of the insulating gas is 0.4 MPa. Under the condition of no wind and solar radiation, the variation of GIL temperature over 10 hours is illustrated in Figure 7. The power losses in the conductor and enclosure are separately 271.27 W/m and 101.12 W/m. In the first three hours, an appreciable increase in the conductor and the enclosure is recognized. During the next seven hours, the temperature rises slow down gradually and nearly come to a steady-state. At the last moment, the temperature rise of the conductor (T_c) is 67 K and that of the enclosure (T_e) is 34K. The accuracy of the results is verified by comparing with measured temperatures reported in [7].

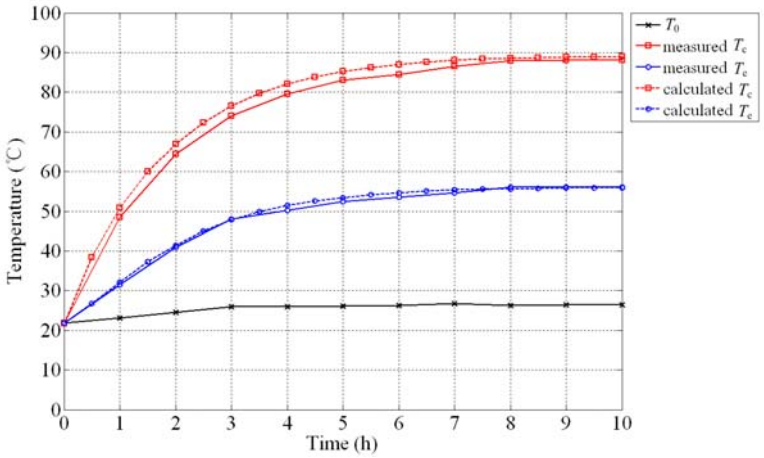

Figure 7. Time variation of calculated GIL temperature

5. Conclusion

In order to investigate the temperature rise of the GIL, a improved FE model has been established. It takes into account the temperature dependent electrical and thermal properties of the materials. Unlike the traditional FEM, the surrounding air is also included in the solution region at the advantage of avoiding convective heat transfer coefficient at the interface of the enclosure and the surrounding air. The multiple species transport technique is used to calculate the temperature distribution.

Both the steady-state and transient temperature rise correspond adequately well with results of measurements reported in the literature. By comparing with the analytical method, and other traditional FEMs which consider constant convective heat transfer coefficient and constant material properties, the proposed model is proved to be more precise. It is believed that the proposed model can be used for better thermal design of GIL and for the real-time temperature prediction of that in service.

References

[1] Benato R, Carlini E M, Mario C D. Gas-insulated transmission lines in railway galleries. *IEEE Transactions on Power Delivery*. 2005; 20(2): 704-709.
[2] Koch H, Schuette A. Gas insulated transmission lines for high power transmission over long distances. *Electric Power System Research*. 1998; 44(1): 69-74.
[3] Kuroyanagi Y, Toya A, Hayashi T. Construction of 8000A class 275kV gas insulated transmission line. *IEEE Transactions on Power Delivery*. 1990; 5(1): 14-20.
[4] Volcker O, Koch H. Insulation co-ordination for gas-insulated transmission lines (GIL). *IEEE Transactions on Power Delivery*. 2001; 16(1): 122-130.
[5] Benato R, Dughiero F, Forzan M. Proximity effect and magnetic field calculation in GIL and in isolated phase bus ducts. *IEEE Transactions on Magnetics*. 2002; 38(2): 781-784.
[6] Hus J. Estimating busbar temperatures. *IEEE Transactions on Industry Applications*. 1990; 26(5): 926-934.
[7] Minaguchi D, Ginuo M, Itaka K. Heat transfer characteristics of gas-insulated transmission lines. *IEEE Transactions on Power Delivery*. 1986; PWRD-1(1): 2-9.
[8] Benato R, Dughiero F. Solution of coupled electromagnetic and thermal problems in gas-insulated transmission lines. *IEEE Transactions on Magnetics*. 2003; 39(3): 1741-1744.
[9] Kim SW, Kim HH, Hahn SC. Coupled finite-element-analytic technique for prediction of temperature rise in power apparatus. *IEEE Transactions on Magnetics*. 2002; 38(2): 921-924.
[10] Kim JK, Hahn SC, Park KY. Temperature rise prediction of EHV GIS bus bar by coupled magnetothermal finite element method. *IEEE Transactions on Magnetics*. 2005; 41(5): 1636-1639.
[11] Hwang CC, Chang JJ, Jiang YH. Analysis of electromagnetic and thermal fields for a bus duct system. *Electric power systems research*. 1998; 45(1): 39-45.
[12] Hedia H, Henrotte F, Meys B. Arrangement of phase and heat constraints in a busbar. *IEEE Transactions on Magnetics*. 1999; 35(3): 1274-1277.
[13] Ho SL, Li Y, Lin X. A 3-D study of eddy current field and temperature rise in a compact bus duct system. *IEEE Transactions on Magnetics*. 2006; 42(4): 987-990.

[14] Ho SL, Li Y, Lin X. Calculations of eddy current, fluid, and thermal fields in an air insulated bus duct system. *IEEE Transactions on Magnetics*. 2007; 43(4): 1433-1436.
[15] Chakir A, Sofiane Y, Aquelet N. Long term test of buried gas insulated transmission lines (GIL). *Applied Thermal Engineering*. 2003; 23(13): 1681-1696.
[16] Anderson JD. Computational Fluid Dynamics: The Basics with Applications. New York: McGraw-Hill. 1995: 452-455.
[17] Zhang YJ, Ruan JJ, Huang T. Calculations of temperature rise in air-cooled induction motors through 3-D coupled electromagnetic fluid-dynamical and thermal finite-element analysis. *IEEE Transactions on Magnetics*. 2012; 48(2): 1047-1050.
[18] Eteiba MB, Aziz MMA, Shazly JH. Heat conduction problems in SF_6 gas cooled-insulated power transformers solved by the finite element method. *IEEE Transactions on Power Delivery*. 2008; 23(3): 1457-1463.